Original Article

THE POTENTIAL ANTICANCER AND NEPHROPROTECTIVE EFFECTS OF FREE OR NANOPARTICLES ENCAPSULATED SITAGLIPTIN IN MOUSE SOLID EHRLICH CARCINOMA

Basma Nabil Saber Ibrahem[1]*, Fleur Fathi Abd El-Moneim[1], Heba Abd-El Galil Aly Mahmoud[1], Gamal Mohamed El Maghraby[2]

[1] Medical Pharmacology Dep., Faculty of Medicine, Tanta University, Tanta, Egypt.
[2] Pharmaceutical Technology Dep., Faculty of Pharmacy, Tanta University, Tanta, Egypt.
Corresponding Author: Basma Nabil Saber Ibrahem, Medical Pharmacology Dep., Faculty of Medicine, Tanta University, Tanta, Egypt.
Email: basma.khalifa@med.tanta.edu.eg

DOI: 10.47750/pnr.2023.14.02.323

Abstract

Background: Breast cancer treatment modalities are in persistent need to be modified due to the rising incidence and associated chemotherapeutics resistance and cytotoxicity. The goal of this work was to evaluate any potential anti-cancerous and nephroprotective effects of sitagliptin either its free form or nanoparticles (NPs) encapsulated form on solid Ehrlich carcinoma in mice. It focused on assessment of nephrotoxicity, drug resistance, apoptosis, oxidative stress, proliferation, and angiogenesis.

Methods: Breast cancer experimental animal model SEC was induced in female albino mice through the subcutaneous implantation of Ehrlich ascites carcinoma (EAC) cells. Mice were randomly divided into 9groups (n=8). Group1 (normal control), group2 (untreated SEC), group3 (SEC +5-FU), group4 (SEC+ SITA), group5 (SEC +SITA-PLGA), group6 (SEC+SITA-Niosome), group7 (SEC+5FU+SITA), group8 (SEC+5FU+SITA-PLGA) and group9 (SEC+5FU+SITA-Niosome). Tumor volume was recorded and on the 28th day post tumor inoculation, mice were sacrificed, blood samples were collected for the assay of BUN and serum creatinine. Tumor was dissected for the assessment of multi-drug resistance-1 (MDR-1), caspase3؛ the other part was prepared for the histopathological examination and immunohistochemical staining of ki67 and VEGF. Moreover, histopathological examination of renal tissue was done.

Results: Administration of sitagliptin augment the anti-cancer properties of 5-FU and showed nephroprotective effects against 5-FU induced nephrotoxicity. Regarding the anticancer effects the nanoparticle formulations of sitagliptin have no significant difference in end tumor volume. however, they showed higher apoptotic properties evidenced by significant increase in the expression of caspase3.

Conclusions: Sitagliptin demonstrated nephroprotective effects which evidenced through significant decrease in BUN and serum creatinine levels and histopathological findings. The nephroprotective properties were augmented by loading sitagliptin on either PLGA or Niosome NPs with superiority to the sitagliptin-niosome NPs.

Keywords: Breast cancer, 5-FU, Sitagliptin, Nephrotoxicity, PLGA, Niosome

Introduction

Breast cancer is the leading cause of female mortality, in 2012, more than half a million deaths were reported and more than 1.7million new cases were diagnosed, which represented about 25% of all newly diagnosed cases [1].

Solid Ehrlich carcinoma (SEC) is a transplantable experimental cancer model corresponding to mammary adenocarcinoma [2], it's implanted in the peritoneal cavity from solid cutaneous or muscular masses allowing growth of standard number of cells to be inoculated subcutaneously and quantify the regression and growth of tumor masses [3].

5-Fluorouracil (5-FU) is a pyrimidine analogue which is considered one of the corner stones in the treatment of various solid tumors due to its broad antitumor activity and synergistic action with other anticancer drugs [4].

Despite the advantages of (5-FU), its clinical application has been limited due to drug resistance and multiple organ toxicity including renal, pulmonary, hematological, cardiac, hepatic, and testicular toxicities [5].

The drug induced nephrotoxicity may be due to the toxic effects of one or more pathological mechanisms including inflammation, tubular cell toxicity, altered hemodynamics, crystals nephropathy and oxidative stress [6].

DPP-4 enzyme is a ubiquitous enzyme expressed on the surface of almost all cell types [7] and is involved in numerous biological activities as modification of many regulatory chemokines or peptides and affecting signaling pathways[8], it also showed apoptogenic and antiproliferative effects against cancer cells [9].

It is important to consider that, one of the key drawbacks of sitagliptin is its short biological half-life in rats, which is just 3.6 hours, and its quick elimination, indicating the need for extremely stringent dose intervals [10].

Recent studies have reported anti-cancerous effects of DPP-4 inhibitors, possibly through their antioxidant, anti-inflammatory properties and increased apoptosis and cell cycle modulation which may represent a novel modality for cancer therapy [11].

Nowadays, the development of nano-sized delivery systems is considered one of the most attractive research areas in the oral drug delivery system that can deliver the appropriate dose to the right place at the appropriate time. Polymeric nano particles (NPS) have been explored for enhancing therapeutic effects, improving patient compliance and limits unwanted systemic adverse effects and toxicity [10, 12].

Nano medicines improve intracellular transport of active pharmaceuticals through binding involving bio-adhesive polymers or chelates; increase their intracellular trafficking when coupled to specific proteins, antibodies, leading to increased membrane permeability, decrease of systemic exposure, higher accumulation in tumor cells. In particular, introduction of such features in anti-cancer agents can improve their efficacy [13].

Material and Methods:

Drugs and chemicals:

5-Flurouracil (Utoral, vial 5mg) from Hikma Specialized Pharmaceuticals company, it was prepared as a solution in saline (i.p.) in a dose of 20mg/kg per day [14, 15], Sitagliptin powder from Glenmark Generics (India) purchased from Andalous Pharma – 6 October city, was prepared as a solution in distilled water and was administered orally by oral gavage either free or loaded on PLGA or niosome nanoparticles in a dose of 10 mg/kg/day [16]. PLGA (Poly (D, L-lactide-co-glycolide) (lactide: glycolide (50:50)), in pellets form, , and Poly vinyl alcohol (PVA) purchased from (Sigma-Aldrich), Acetone (LAXESS-India), Glycerol mono-oleate (Peceol) from gattefosse, Saint-Priest Cedex, France, Sorbitan monostearate (span 60), Cholesterol and ethanol.

Preparation of sitagliptin-PLGA nanoparticles:

PLGA (100mg) was dissolved in 1.5ml of dichloromethane. Sitagliptin (10mg) was dissolved in 0.3ml of water and 0.2 ml of acetone was added to this solution. This mixture was homogenized for 5 minutes using (Polytron

homogenizer, PT-MR 3100, Kinematica AG, Littau-Switzerland) to prepare water in oil nano-emulsion. Then 4ml of PVA aqueous solution (4% w/v) was mixed with the preformed nano-emulsion and the resulted mixture was similarly homogenized for another 5 minutes at the end of which the developed emulsion was mixed with 6ml of PVA solution (0.5% w/v), the developed system was kept overnight under continuous magnetic stirring allowing the evaporation of the organic solvent depositing the PLGA nanoparticles **[17]**.

Preparation of sitagliptin-niosome nanoparticles:

Niosomes were prepared by the hydration of proniosomes [18]. Span 60, peceol, cholesterol and sitagliptin were heated on a thermostated water bath, a clear liquid was developed after the addition of ethanol. 2ml of water was added to the mixture while continuous mixing on the water bath to form homogenous dispersion. The proniosomes were developed from stirring the dispersion away from the water bath. The proniosomes were hydrated gradually with water while mixing to develop the crude niosomes which were kept overnight at ambient temperature allowing complete swelling. To reduce the vesicle size, the swollen vesicles were then subjected for sonication for 1 hour **[19]**.

Induction of Solid Ehrlich carcinoma (SEC) model:

The initially inoculated EAC cells was provided by the National Cancer Institute (Cairo University, Egypt) and propagated by weekly intraperitoneal (i.p) injection of $2.5x10^6$ cells per mouse. [20] . EAC cells can grow in both solid and ascitic forms. The ascitic form was done by intraperitoneal (i.p.) transplantation of 2.5×10^6 EAC cells in two mice and allowed to multiply where an ascitic fluid containing Ehrlich tumor cells developed within 10 days. Then, the ascitic fluid was withdrawn by a sterile syringe, diluted in 0.9% sterile saline (1:9 v/v) and counted using a Neubauer Hemocytometer. The cell viability was determined by trypan blue dye exclusion method and was found to be more than 99%. In order to develop Ehrlich solid tumor, all animals were subcutaneously inoculated with (0.2ml/mice) that contained 2.5×10^6 viable EAC cells, in the back of each female mouse **[21-24]**.

Animals groups and study design:

The study was performed on 72 female Swiss albino mice weighing 20-25 g, injected by 0.2ml of 2.5×10^6 viable EAC cells in the back of each mouse and left for 12 days. The treatment protocol was started on the 12^{th} day post subcutaneous tumor implantation and was continued for 16 days (28^{th} day post tumor implantation). The animals were kept in wire mesh cages at the animal laboratory room in the Pharmacology department under constrict hygienic measures with free access to fresh water and standard animal diet *ad libitum.* One week before the induction of tumors, the animals were kept for acclimatization to the housing environment

Animals were randomly divided into 9 equal groups: group 1(normal control: had free access to fresh water and standard animal diet *ad libitum* and received a daily vehicle of distilled water by oral gavage and injected i.p. by normal saline till the end of the experiment, group 2 (untreated SEC): animals were subcutaneously implanted by Ehrlich tumor cells into the back [22-24] and started to receive a daily vehicle of distilled water by oral gavage and injected i.p. by normal saline, group3: SEC group treated with 5-FU [14, 15], group4: SEC group treated with free sitagliptin [16], group5: SEC group treated with SITA-PLGA nanoparticles (NPs), group 6: SEC group treated with niosomal SITA NPs by, group7: SEC group treated with combination of 5-FU and free sitagliptin, group8: SEC group treated with combination of 5-FU and SITA-PLGA NPs and group9: SEC group treated with combination of 5-FU and niosomal SITA NPs. The treatment protocol was started from the 12^{th} day post tumor implantation and continued to the end of the experiment at the 28^{th} day post tumor implantation.

Tumor volume:

Tumor sizes were assessed and recorded using Vernier caliper at the (12^{th}, 16^{th}, 20^{th}, 24^{th} and 28^{th}) days post implantation and the tumor volumes were calculated according to the following formula: Tumor volume $= {}^{1}/_{2} \, (length \times width^2)$ [25].

Blood and tissue sampling and processing:

At the end point of the experiment (28th day post tumor implantation), all survived mice were sacrificed. Blood samples were collected and centrifuged to assess blood urea nitrogen (BUN) and serum creatinine levels were measured by spectrophotometer utilizing Biodiagnostic company's kits. Tumor masses were dissected and washed with phosphate-buffered saline (PBS) solution, pH 7.4 to remove any red blood cells and clots, and divided into two **parts, the first** was homogenized as 1gm tumor tissue in 5 ml cold PBS pH 7.4 then centrifuged at 4000 rpm for 15 min at 4° C, and the resultant supernatant was frozen at -80°C for the assay of: Multidrug resistance protein-1(MDR-1) by ELISA kit from Sun Red; Catalogue No. 201-02-1958,and Caspase-3 levels by ELISA kit from Sun Red; catalogue No 201-02-0446, the second part was fixed in 10% formalin and was processed for the histopathological examination (H&E) and immunohistochemical staining of vascular endothelial growth factor (VEGF) and of Ki-67. The kidney was also dissected and washed with saline and fixed in 10% neutral buffered formalin (pH 7.4) for histopathological examination (H&E).

Immunohistochemical expression of VEGF: was done using mouse VEGF polyclonal antibody purchased from Invitrogen, Thermo scientific, Catalog number (PA1-21796). Staining was performed on formalin-fixed paraffin-embedded specimens for vascular endothelial growth factor (VEGF ready to use for IHC, 1467-R7)

Interpretation of VEGF IHC staining:

Immunostaining for VEGF was judged positive when tumour cells had unambiguous cytoplasmic staining with or without nuclear staining. Quantitative evaluation of VEGF staining density was performed as follows: Negative (-) scores were assigned to specimens with sparse or no staining or less than 10% staining. Greater than 10% but less than 25% of the staining was rated as weak (+). > 25%, but < 75% of the staining was rated as moderate (++), whereas > 75% was rated as strong (+++). Necrotic cell staining was judged negative **[26].**

Immunohistochemical expression of tissue Ki-67:

The Ki-67 antibodies were obtained from Invitrogen, Thermo scientific, Catalogue number (MA5-14520). Ki-67 monoclonal antibodies were diluted in 10mM of phosphate buffer saline, pH 7.2 with 1% bovine serum albumin and 0.1% sodium azide.

Interpretation of Ki-67 IHC staining:

Ki-67 score was reported as the proportion of immunostained nuclei relative to the total number of tumour cell nuclei, irrespective of immunostaining strength. The counting was conducted at x400 magnification in three randomly selected areas of the tumour tissue slice. Ki-67 scores varied from 0% to 100%, and the threshold for a positive result was 14%. Ki-67 expression is classified into three groups: low (Ki-67 15%), intermediate (Ki-67:16-30%), and high (Ki-67 > 30%). Necrotic cell staining was judged negative [27].

Ethical approval: The work was approved by "Research Ethics Committee, REC", Faculty of Medicine, Tanta University, Egypt (Approval no.#33390/10/19).

Statistical analysis:

The obtained values were statistically evaluated using version 22 for Windows® (SPSS Inc, Chicago, IL, USA). Shapiro-Wilks normality test and histograms were used to test the distribution. Parametric variables were expressed as mean and standard deviation (SD) and were compared using ANOVA test among the groups with post hoc (Tukey) test. The software (Image J) (National Institute of Health, Bethesda, Maryland, USA) [28] was used to estimate the tumor necrotic areas then data were analyzed by one way analysis of variance (ANOVA) test followed by Post Hoc Tukey's test. P value ≤ 0.05 was considered statistically significant.

Results:

Characterization of prepared nano-formulations by transmission electron microscopy (TEM):

The TEM micrographs revealed nearly spherical shape and average particles size was calculated to be 114.56 ± 32.72 nm for sitagliptin-PLGA nanoparticles and 58.64 ± 9.16 nm for sitagliptin-niosome nanoparticles. The recorded size data were obtained from 10 recorded measurements (n=10). Figure 3

Figure 3: A- TEM of sitagliptin-PLGA nanoparticles, B- TEM of sitagliptin-niosome nanoparticles

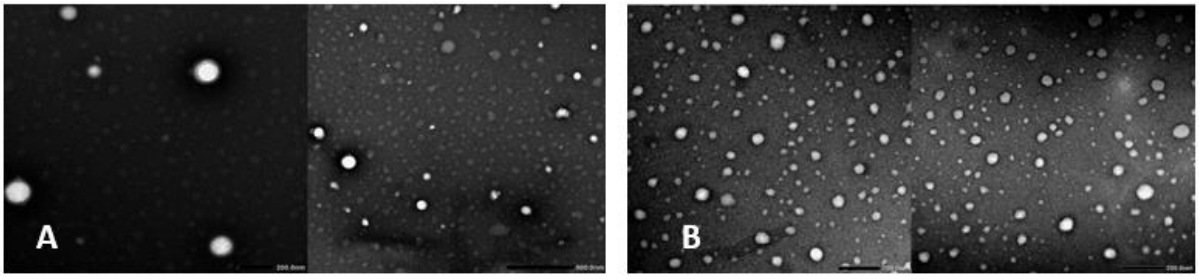

Tumor volume (mm^3) at the end experimental point 28th day post implantation:

Group3 showed a significant shrinkage in tumor mass versus group2. Group4, group5 and group6 showed significant shrinkage in tumor mass versus group2 and significant increase in tumor volume versus group3. Group7, group8 or group9 showed significant shrinkage in tumor mass versus group3. Insignificant changes in tumor volume in group7, group8 and group9. Table 2

Fig 4: Tumor volume at end experiment point (28th day post implantation)

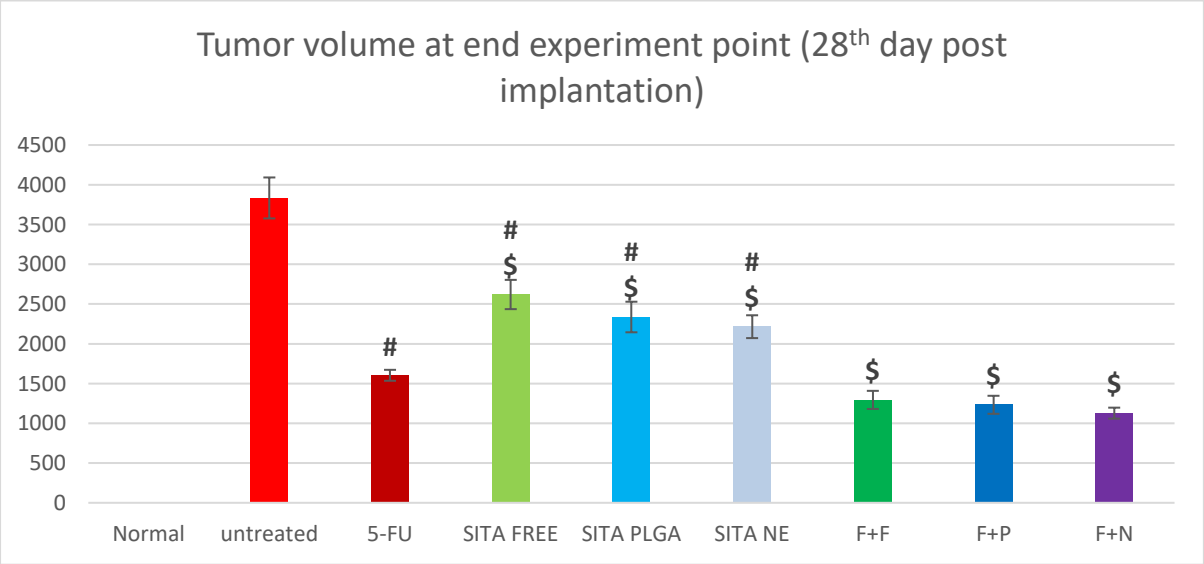

 # Significant difference from untreated SEC group (group2) , $ Significant difference from SEC treated group with 5FU (group3)

Table 1: Time course of the volume of solid Ehrlich carcinoma (mm^3):

Days after implantation	Group2 SEC	Group3 5FU	Group4 SITA free	Group5 SITA PLGA	Group6 SITA niosome	Group7 5FU+SITA free	Group8 5FU+ SITA PLGA	Group9 5FU+ SITA niosome
12th day	123.47 ± 36.35	122.68 ± 24.94	121.57 ± 16.57	124.25 ± 9.94	126.66 ± 22.31	125.98 ± 32.55	122.81 ± 18.55	121.22 ± 22.69
16th day	992.01 ± 117.03	566.02 ± 72.91	784.87 ± 69.75	741.42 ± 122.88	687.41 ± 72.44	549.46 ± 93.70	532.82 ± 70.97	519.47 ± 151.61
20th day	2011.87 ± 274.86	1040.97 ± 91.69	1421.78 ± 163.66	1288.4 ± 128.77	1217.41 ± 79.57	958.96 ± 77.33	852.85 ± 110.38	817.28 ± 119.85
24th day	2643.01 ± 84.10	1408.71 ± 86.56	1915.18 ± 175.10	1717.73 ± 76.17	1589.23 ± 170.72	1136.67 ± 126.36	1056.97 ± 116.11	1009.05 ± 105.26
28th day	3438.42±2 57.60	1603.76± 68.78	2620.13± 183.10	2336.94±19 2.28	2215.27±13 4.63	1294.48±11 3.86	1232.78± 133.48	1127.72± 69.18

Data is presented as mean ± SD, Significant difference < 0.05.

Serum blood urea nitrogen (BUN) (mg/dl) and creatinine (mg/dl) levels:

Group3, group7, group8 and group9 demonstrated significant rise in serum BUN versus either group1 or group2. Group7, group8 and group9 demonstrated significant decline in serum BUN versus group3. Group8 and group9 demonstrated notable decline in serum BUN versus group7. Group9 showed a significant decrease in serum BUN levels versus group8. Figure 5

Regarding serum creatinine levels Group3, group7, group8 and group9 demonstrated significant rise in serum creatinine levels versus either group1 or group2. Group7 and group8 and group9 significantly decrease versus group3. Figure 6.

Fig. 5: Serum blood urea nitrogen (BUN) (mg/dl) levels

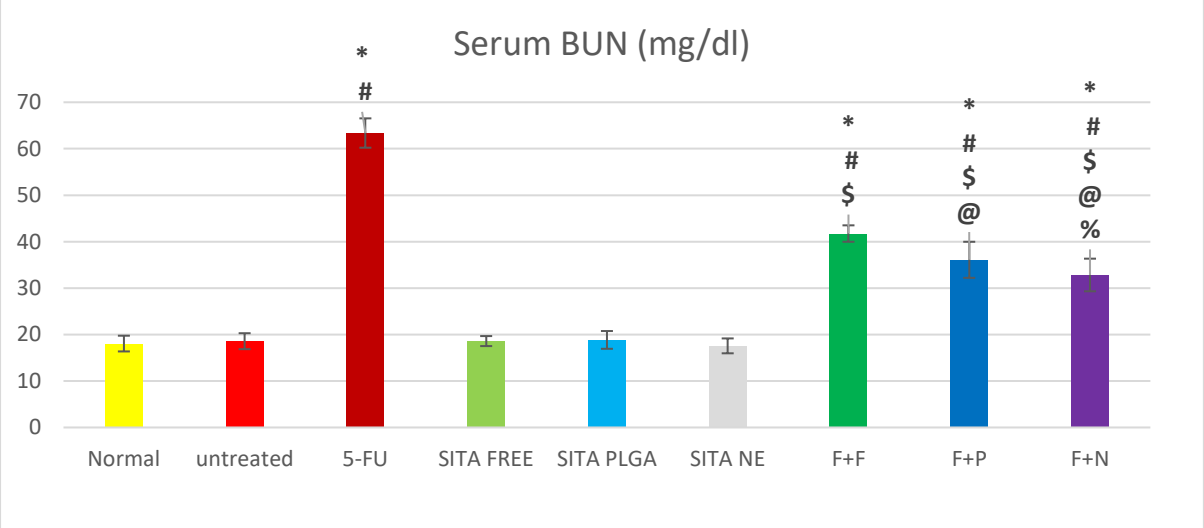

* Significant difference from normal control group (group1), # Significant difference from untreated SEC group (group2) ,$ Significant difference from SEC treated group with 5FU (group3) , @Significant difference from SEC treated group with 5FU+ free sitagliptin (group7) , %Significant difference from SEC treated group with 5FU+ SITA PLGA NPs (group8)

Fig. 6: Serum creatinine levels (mg/dl)

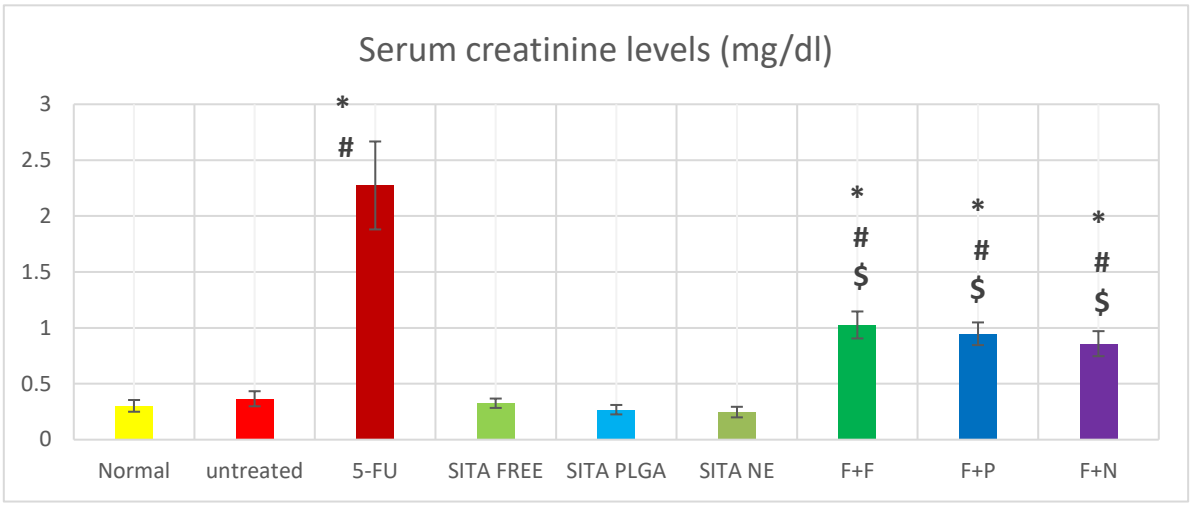

* Significant difference from normal control group (group1), # Significant difference from untreated SEC group (group2), $ Significant difference from SEC treated group with 5FU (group3)

Tumor tissue Multidrug resistance protein-1(MDR-1) levels (ng/ml):

Group3, group7, group8 and group9 demonstrated significant declines versus group2. Group7, group8 or group9 demonstrated significant rise versus group3 (Figure 7).

Fig. 7: Tumor tissue MDR-1 levels (ng/ml)

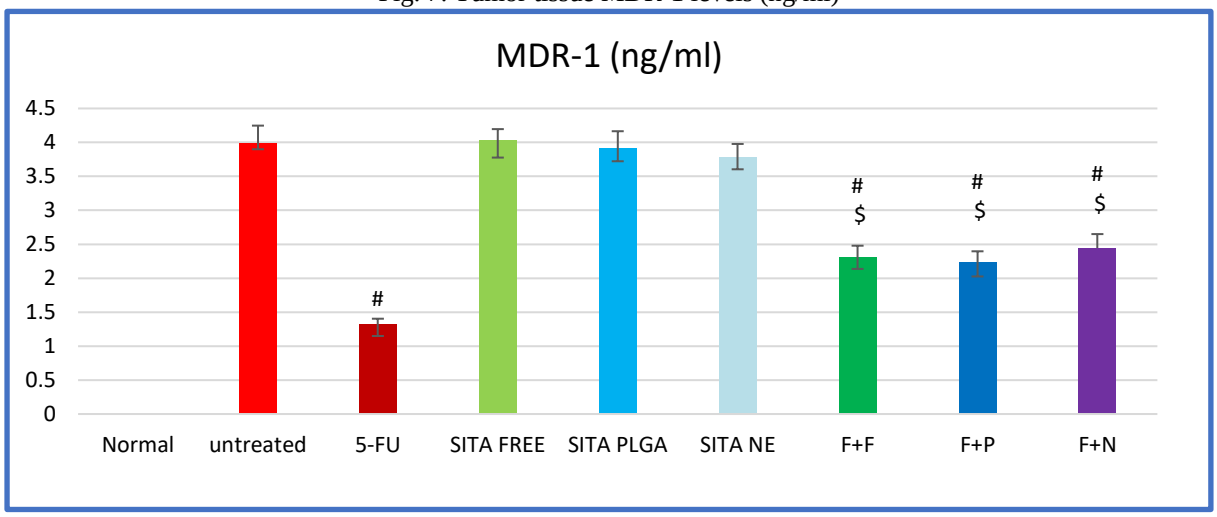

Significant difference from untreated SEC group (group2), **$** Significant difference from SEC treated group with 5FU (group3)

Tumor tissue Caspase-3 levels (ng/ml):

Group3 showed a significant increase in caspase-3 tissue level versus group2. Group4, group5, group6, group7, group8 or group9 demonstrated significant rise versus group2. Group4, group5, group6 demonstrated significant decline versus group3. Group5 and group6 demonstrated significant rise versus treated group4. Group6 demonstrated significant rise versus group5. Group7, group8 and group9 demonstrated significantrise versus group3.. Figure 8.

Fig. 8: Tumor tissue caspase-3 levels (ng/ml) at different studied groups.

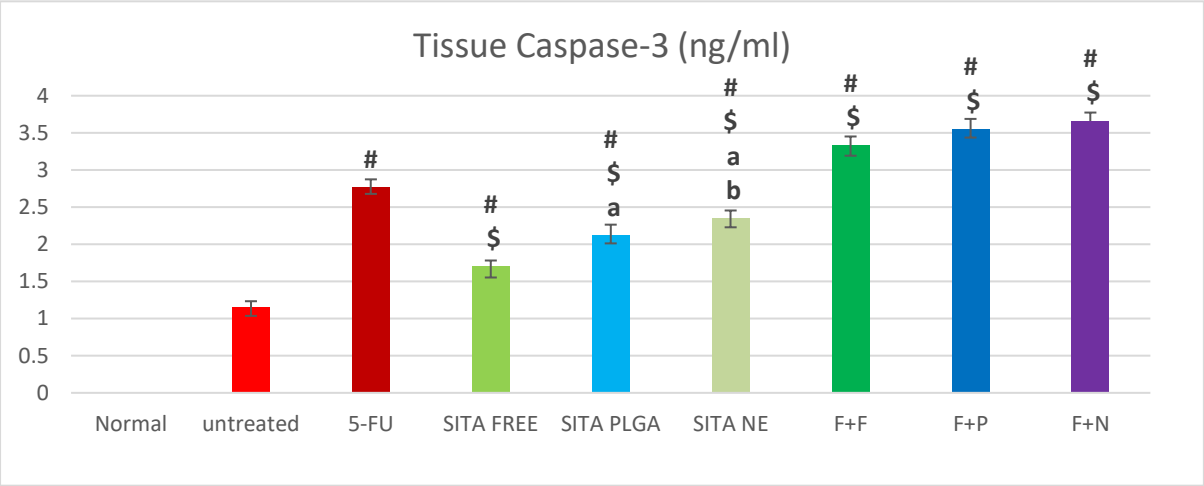

Significant difference from untreated SEC group (group2), **$** Significant difference from SEC treated group with 5FU (group3), a Significant different from SEC treated with sitagliptin (group4), b Significant different from SEC treated with sitagliptin-PLGA (group5)

Histopathological examination as shown in Figure 9:

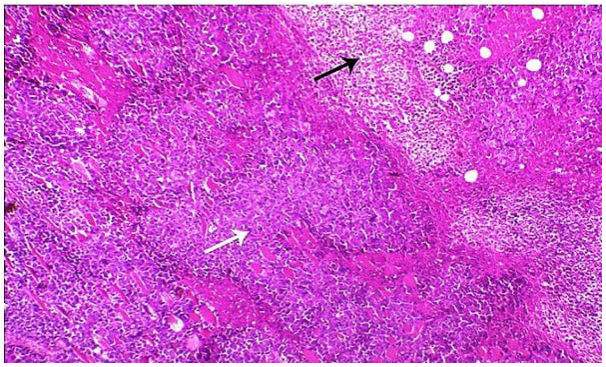

(A)

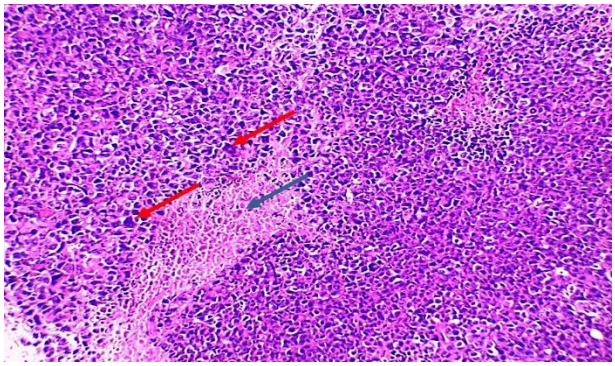

(B)

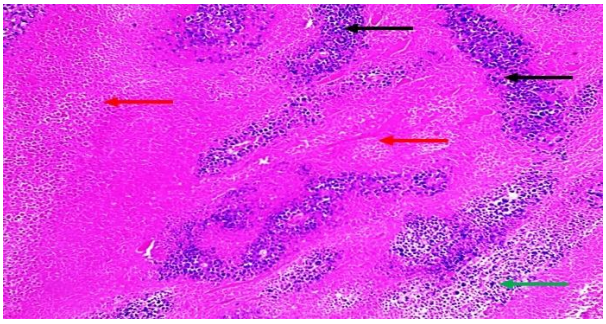

(C)

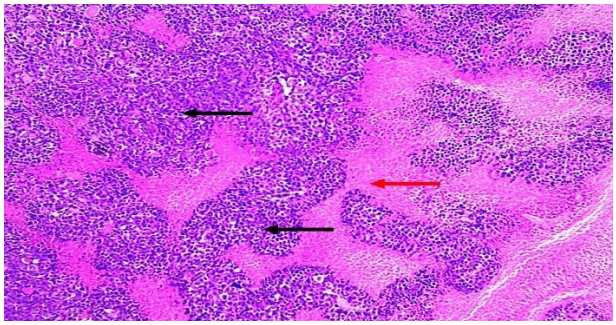

(D)

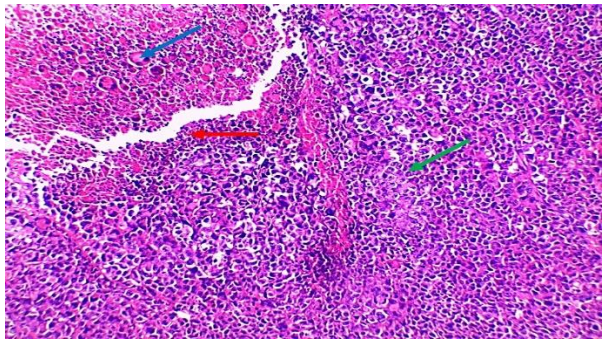

(E)

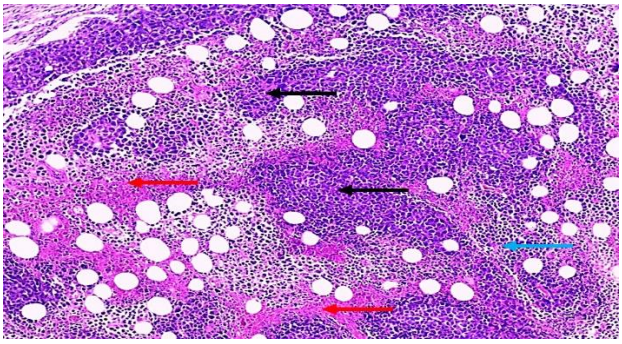

(F)

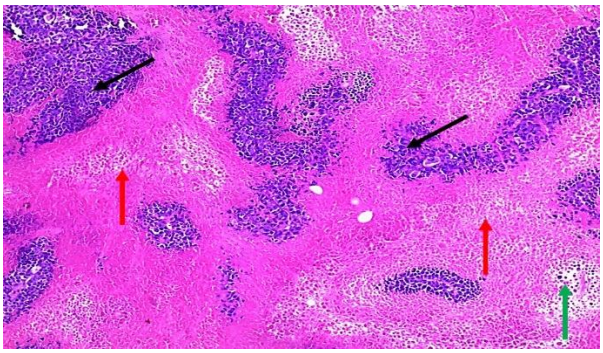

(G)

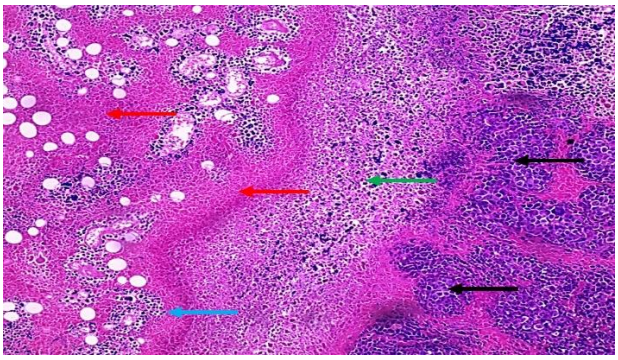

(H)

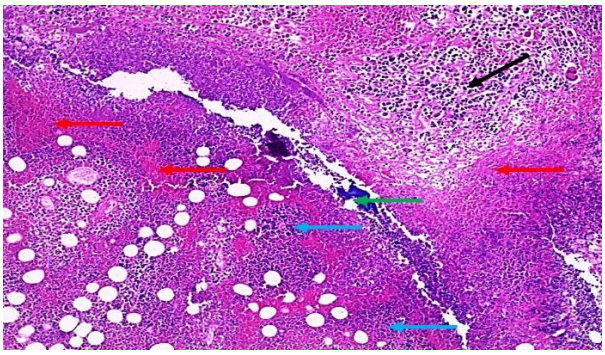

(I)

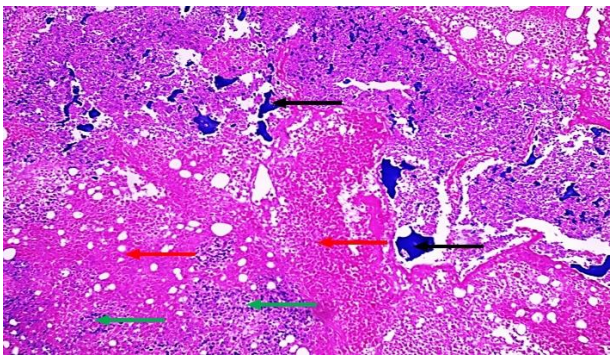

(J)

Figure 9: **(A)** group2 showed wide area of proliferation of neoplastic cells (white arrow) with limited central necrosis (black arrow) (H&E X100), **(B)** H&E (X200) stained tumor section from group2 showed solid sheets of cancerous cells exhibiting pleomorphism, hyperchromatism and abnormal mitotic figures (red arrows) and focal area of necrosis (blue arrow), **(C)** group3 exhibited cancerous cells (black arrows) surrounded by 70% of necrotic cancerous cells (red arrows) and moderate lymphocytic infiltrate (green arrow) (H&E X 100), **(D)** group4 exhibited cancerous cells (black arrows) surrounded by 20% of necrotic cancerous cells (red arrow) (H&E X 100), **(E)**: group4 showed focal area of necrosis containing vacuolar degeneration of cancerous cells (blue arrow), mild interstitial lymphocytic infiltrate (blue arrow) surrounded by cancerous cells (green arrow). (H&E X 200), **(F)**: group5 exhibited cancerous cells (black arrows) surrounded by 40% of necrotic cancerous cells (red arrows) and mild lymphocytic infiltrate (blue arrow) (H&E X 100), **(G**): group6 exhibited cancerous cells (black arrows) surrounded by 60% of necrotic cancerous cells (red arrows) and mild lymphocytic infiltrate (green arrow) (H&E X 100), **(H)**: group7 exhibited cancerous cells (black arrows) surrounded by 75% of necrotic cancerous cells (red arrows) and moderate lymphocytic infiltrate (blue arrow) with foci of calcifications (green arrow) (H&E X 100), **(I):** group8 exhibited cancerous cells (black arrow) surrounded by 90% of necrotic cancerous cells (red arrow)

and marked lymphocytic infiltrate (blue arrows) with foci of calcifications (green arrow) (H&E X 100), **(J):** group9 showed few cancerous cells surrounded by 95% of necrotic cancerous cells (red arrows) and marked lymphocytic infiltrate (green arrows) with foci of calcifications (black arrows) (H&E X 100)

Tumor tissue necrosis percentage:

Group3 showed a significant increase versus group2. Group4, group5 and group6 demonstrated significant decline versus group3. Group7, group8 and group9 demonstrated significant rise versus group3.. Figure 10

Fig. 10: Tumor tissue necrosis percentage in different studied groups

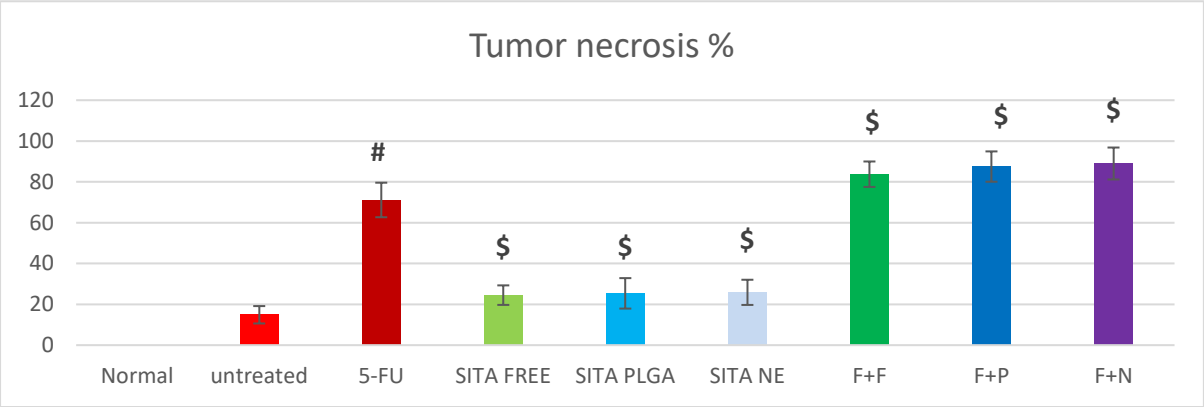

Significant difference from untreated SEC group (group2), **$** Significant difference from SEC treated group with 5FU (group3)

IHC staining and scoring of VEGF:

IHC staining of VEGF (Figure 11).

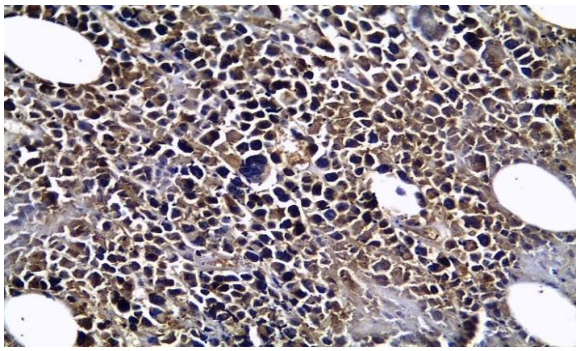

(A)

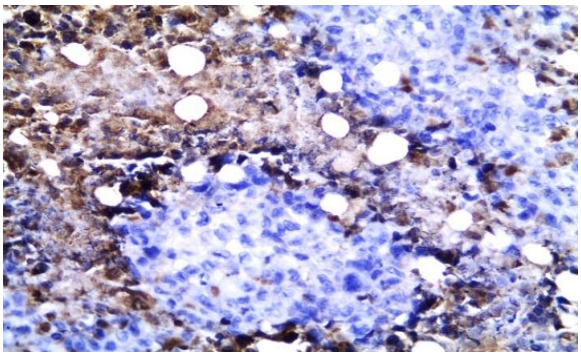

(B)

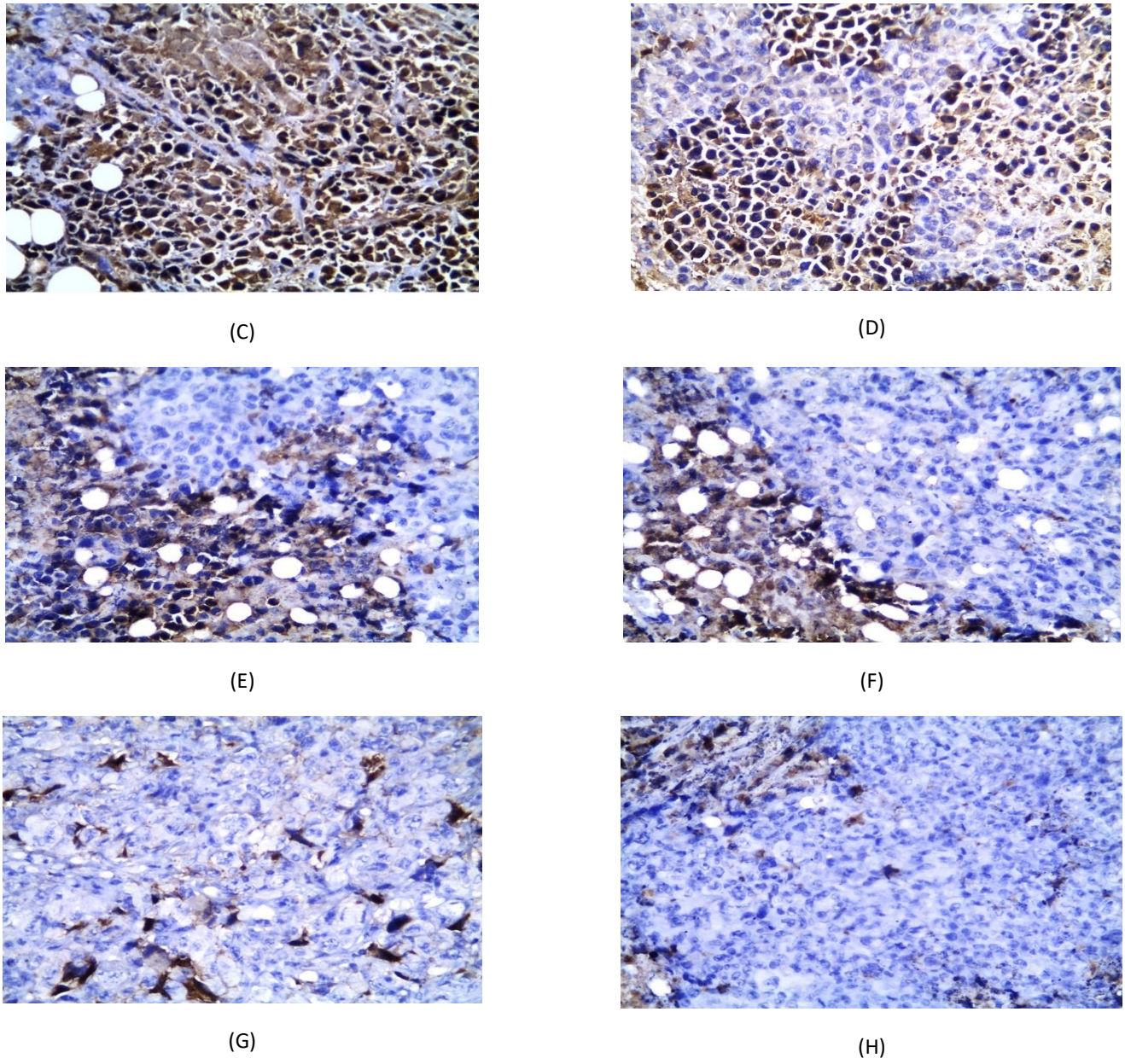

Fig. 11: (A): group2 showed strong positive VEGF expression in more than 75% of cancerous cells (H&E X 400), **(B):** group3 showed weak positive VEGF expression in 35% of cancerous cells (H&E X 400). Fig.**(C):** group4 showed strong positive VEGF expression in more than 70% of cancerous cells (H&E X 400). **(D):** group5 showed moderate positive VEGF expression in 68% of cancerous cells (H&E X 400). **(E):** group6 showed moderate positive VEGF expression in 65% of cancerous cells (H&E X 400). **(F):** group7 showed weak positive VEGF expression in 20% of cancerous cells (H&E X 400). **(G):** group8 showed weak positive VEGF expression in 15% of cancerous cells (H&E X 400). **(H):** group9 showed weak positive VEGF expression in 15% of cancerous cells (H&E X 400).

IHC expression of VEGF percentag:

Group3 showed a significant decrease in VEGF expression versus group2. Group4, group5 and group6 demonstrated significant decline in VEGF expression versus group2 and significant increase versus group3. Group7, group8 and group9 demonstrated significant decline in VEGF expression versus group3.. Figure 12

Fig. 12: Tumor tissue expression of VEGF %

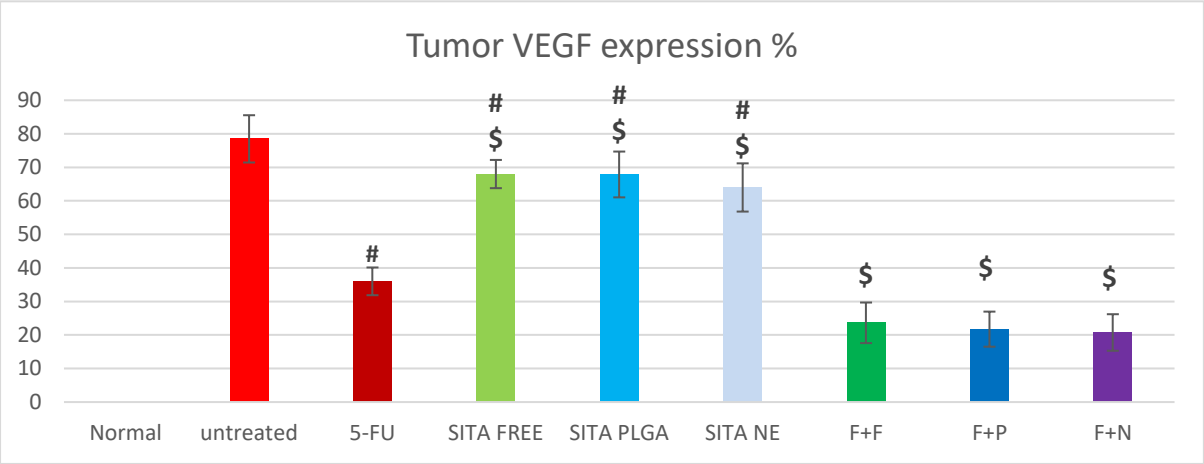

Significant difference from untreated SEC group (group2), **$** Significant difference from SEC treated group with 5FU (group3)

IHC staining and scoring of ki67:

ki-67 staining (Figure 13)

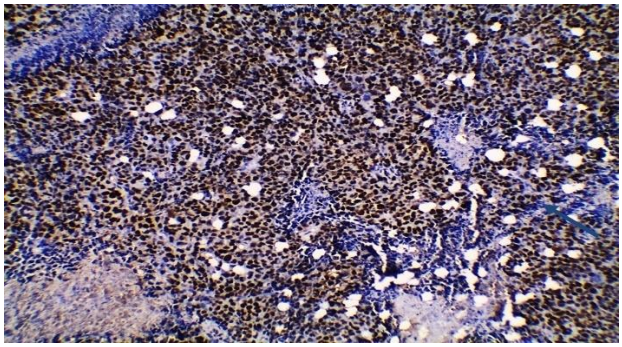

(A)

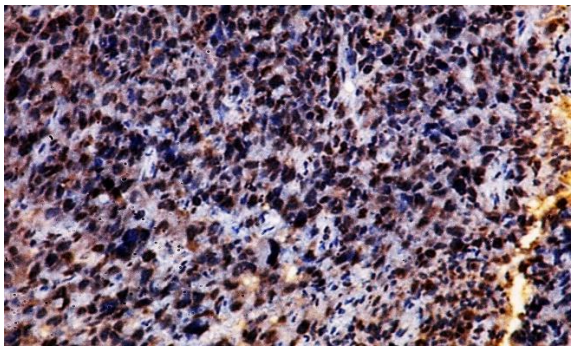

(B)

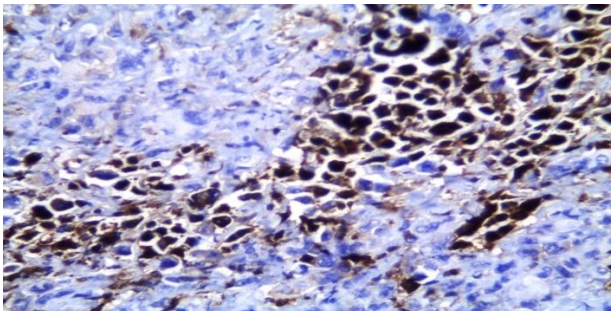

(C)

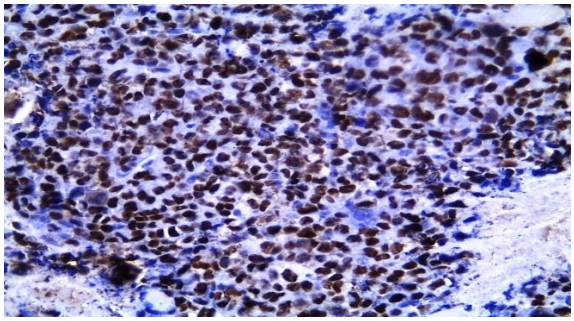

(D)

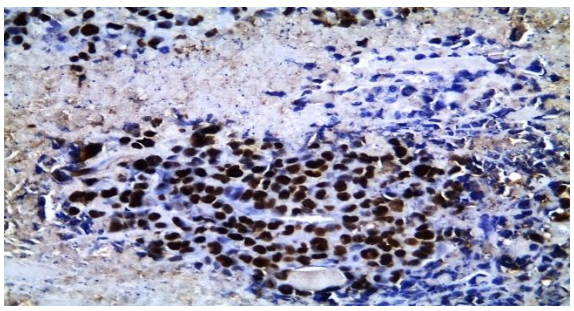

(E)

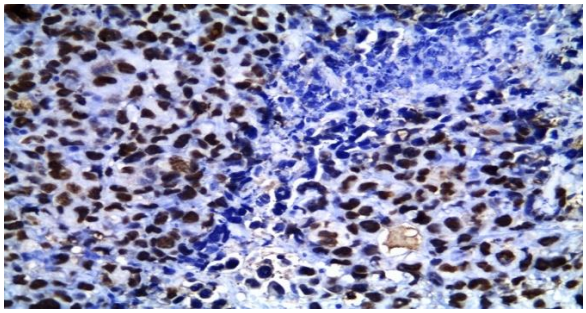

(F)

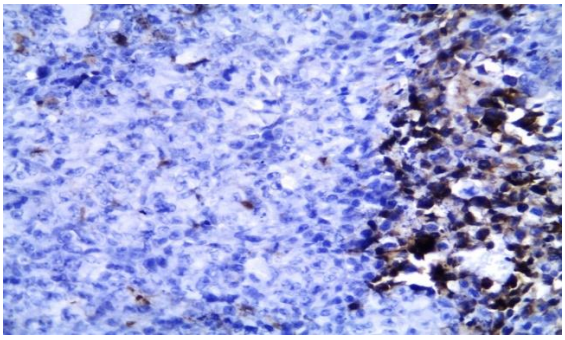

(G)

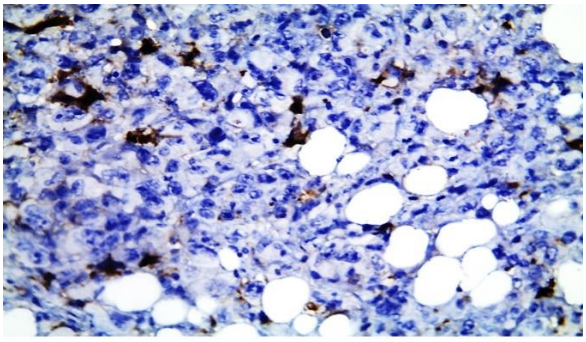

(H)

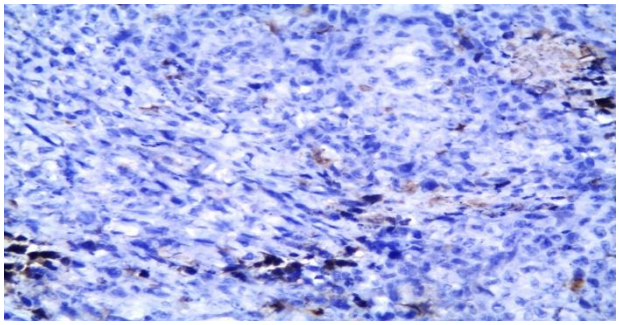

(I)

Fig. 13: **(A):** Group2 showed high Ki-67 proliferation index expression in cancerous cells (H&E X 200), **(B)**: group2 Higher magnification showed high Ki-67 proliferation index expression in cancerous cells 80% (H&E X 400), **(C):** group3 showed intermediate Ki-67 proliferation index expression in cancerous cells 30% (H&E X 400), **(D):** group4 showed high Ki-67 proliferation index expression in cancerous cells 70% (H&E X 400), **(E):** group5 showed intermediate Ki-67 proliferation index expression in cancerous cells 65% (H&E X 400), **(F):** group6 showed Ki-67 proliferation index expression in cancerous cells 65% (H&E X 400), **(G):** group7 showed Ki-67 proliferation index expression in cancerous cells 20% (H&E X 400). **(H):** group8 showed Ki-67 proliferation index expression in cancerous cells 15% (H&E X 400), **(I):** group9 showed Ki-67 proliferation index expression in cancerous cells 15% (H&E X 400).

IHC expression of Ki67 percentage:

Group3 showed a significant decrease in ki67 expression versus group2. Group4, group5 and group6 demonstrated significant decline in ki67 expression versus group2 and significant increase versus group3. Group7, group8 and group9 demonstrated significant decline in ki67 expression versus group3.. Figure 14

Fig. 14: Tumor tissue ki67 expression %

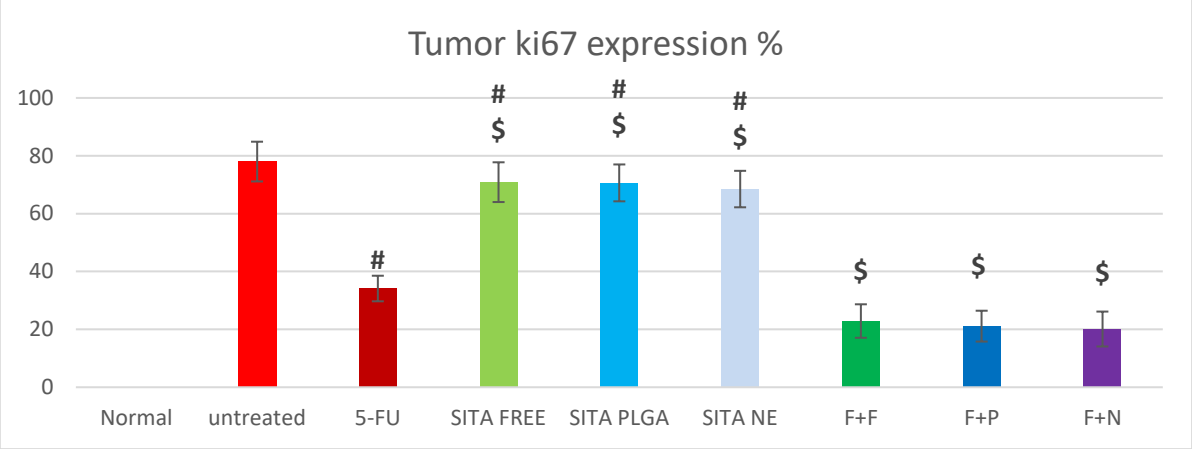

Significant difference from untreated SEC group (group2), **$** Significant difference from SEC treated group with 5FU (group3)

Histopathological examination of kidney: as shown in Figure 15

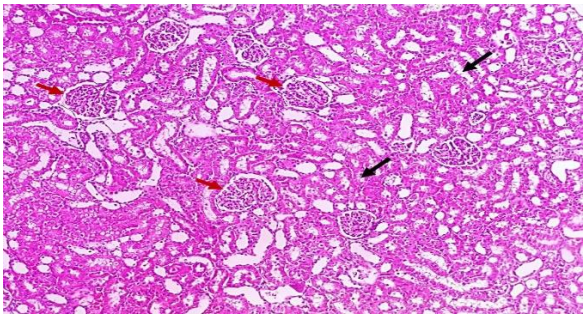

(A)

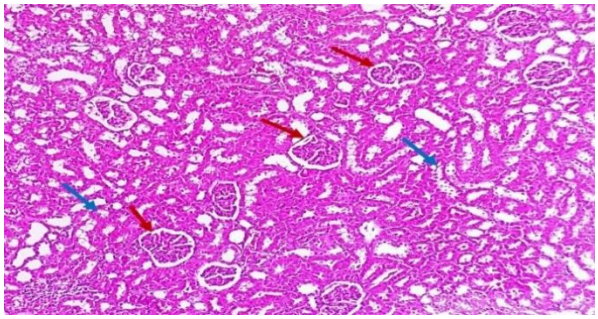

(B)

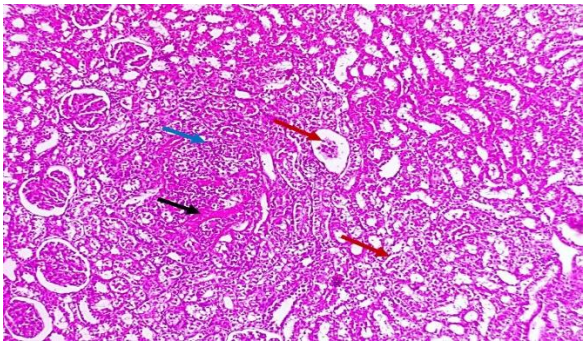

(C)

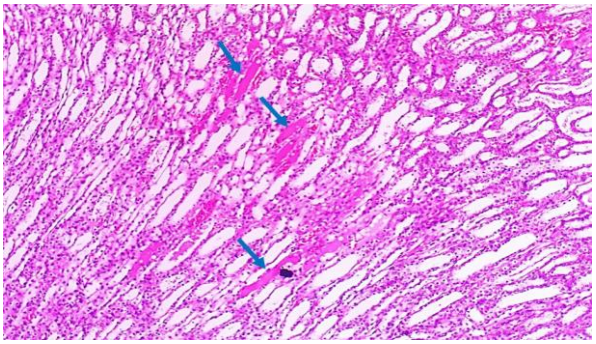

(D)

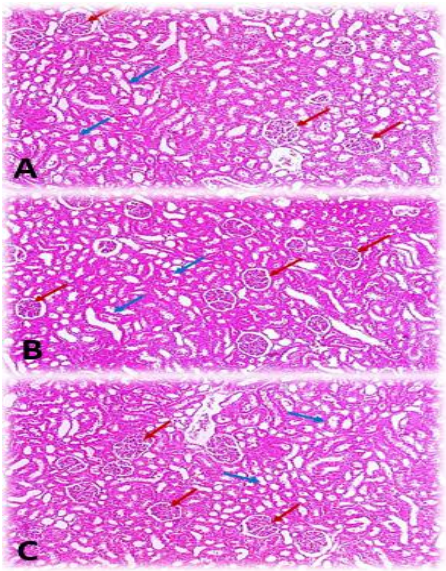

(E)

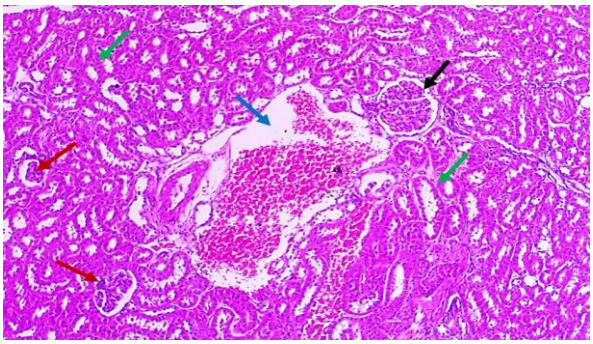

(F)

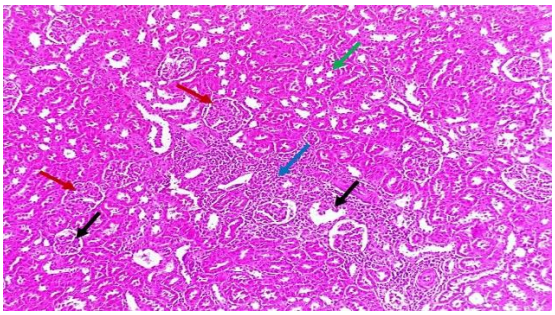

(G)

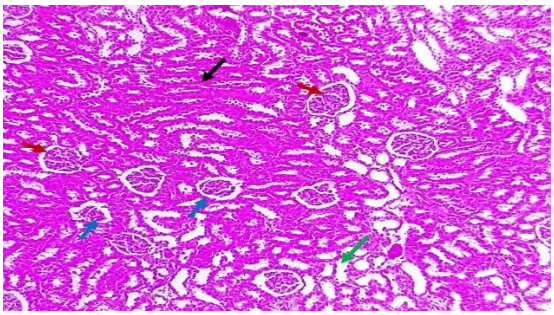

(H)

Fig. 15: (A): Normally shaped glomeruli (red arrows) surrounded by normally shaped tubules lined with columnar cells (black arrows) [H and E X 100], **(B):** normally shaped glomeruli (red arrows) surrounded by normally shaped tubules lined with columnar cells (blue arrows) [H and E X 100], **(C):** Focal area of necrosis (black arrow) surrounded by chronic inflammatory cellular infiltrate (blue arrow) and some small atrophic glomeruli (red arrows) [H and E X 100], (**D):** Dilated tubules, some of them filled with hyaline casts (blue arrows) [H and E X 100], **(E):** group4 A, sitagliptin PLGA NPs (group5) B and sitagliptin niosome NPs (group6) C, showed normally shaped glomeruli (red arrows) surrounded by normally shaped tubules lined with columnar cells (blue arrows) [H and E X 100], **(F):** Congested vessel (blue arrow) surrounded by many atrophic glomeruli (red arrows) and some normally shaped glomeruli (black arrow) and normally shaped tubules (green arrows) [H and E X 100], **(G):** Normally shaped glomeruli (red arrows) and some atrophic glomeruli (black arrows) surrounded by focal chronic inflammation (blue arrow) and normally shaped tubules (green arrow) [H and E X 100], **(H):** Normally shaped glomeruli (red arrows) and few atrophic glomeruli (blue arrows) surrounded by normally shaped tubules (green arrow) and some showing focal hyalinization (black arrow), no inflammation or necrosis [H and E X 100].

Discussion

The present study demonstrated that the implantation of EAC cells in female mice developed SEC with gradual increase in tumor mass volume in the subsequent 12 days post-implantation.

Also, the histopathological evaluation of SEC sections showed neoplastic mass with sheets of cancerous cells exhibiting pleomorphism, hyperchromatism and abnormal mitotic figures higher representing cell proliferation surrounding few areas of necrosis and differentiated cells.

In the present study, the end tumor volume of the untreated SEC bearing mice showed positive correlations with MDR-1, tissue MDA, tissue expression of ki67 and VEGF and negative correlations with tissue caspase3, tissue GSH and tissue necrosis.

The fluoropyrimidine 5FU is still currently widely used for treatment of various solid tumors including BC [29].

It is a pyrimidine antimetabolite analogue that interferes with the nucleoside metabolism which is incorporated into RNA and DNA leading to cell death. Because of its high metabolic rate into the body, the maintenance of therapeutic serum concentration requires the continuous administration of high dose that leads to severe toxic effects. Also, the development of cellular resistant against 5FU is one of the main causes that greatly limited its clinical application [30].

In the present study, the treated SEC bearing mice with 5FU demonstrated notable decline in end tumor volume, significant decrease in MDR-1, significant increase in caspase3, significant decrease in GSH levels, significant increase in MDA levels, significant increase in necrosis percentage, significant decrease in ki67 expression and significant decrease in VEGF expression when compared to untreated SEC bearing mice received daily vehicle.

The present study is in harmony with Soliman et al. [31] who reported that 5FU mediate its anti-cancerous effects through nucleic acids damage, over expression of tumor suppressor gene p53 and the release of ribosome-free rpL3 through the induction of nuclear stress which acts as pro-apoptotic factor.

Meanwhile Gaballah et al. [15] demonstrated that the treatment with 5FU increased the beclin-1 levels inducing the production of autophagosomes triggering the autophagic process in cancer cells.

Multiple drug resistance (MDR) is the fundamental obstacle facing the chemotherapeutic treatment of breast cancer in which cancer cells acquiring cross-resistance to unrelated chemotherapeutic drugs following exposure to a certain cytotoxic medication. One of the major mechanisms of MDR is the actively extruding drugs out of cells through a group of ATP-binding cassette (ABC) transporter proteins that functions as efflux pumps [32].

P-glycoprotein (P-gp), which is expressed by the MDR1 (ABCB1) gene, has been the subject of the most research about its capacity to produce MDR phenotype.

In addition to MDR it shows additional functions as promoting cellular proliferation and inhibiting apoptosis during cancer progression. The over expression of P-gp is correlated with more aggressive malignancies phenotypes with poor prognosis [33].

In this context, the treated SEC bearing mice with 5FU demonstrated notable decline in MDR-1 levels, these results are in accordance with Ma et al. [34] who reported that the 5FU in metronomic therapy can target the cancer associated fibroblasts (CAFs) reversing the MDR through their sensitization and down regulation of P-gp expression.

Also, Inoue et al. [35] have reported that the pretreatment of cancer colon cell line with 5FU downregulated MDR1 mRNA expression with subsequent enhancement of irinotecan cytotoxicity.

Apoptosis is considered the corner stone in abnormal cell growth and development. Caspase signaling cascade is one of the pathways implemented in apoptosis. The expression and/or activation of caspase signaling cascade have been implicated in various malignancies in which loss of caspases promotes tumor development [36].

Caspase3 an executioner caspase is the central member of the cysteine-aspartic acid protease (caspase) family that plays a dominant role in the apoptotic signaling pathway and to regulate cellular apoptosis. The most important substrate of caspase3 is poly (ADP-ribose) polymerase1 (PARP-1) which is responsible for DNA repair and programmed cell death and the cleavage of caspase3 during the early stages of apoptosis into 29 and 85-KDa fragments. This cleavage is responsible for tumor repopulation in apoptotic tumor cells. The changes in the

expression of caspase3 is related to the prognosis and tumorigenesis of many malignancies including breast cancer *[37]*.

Regarding apoptosis, the treated SEC bearing mice with 5FU demonstrated notable rise in caspase3 levels, these results were in accordance with Ponce-Cusi and Calaf [38]who proved the apoptotic activity of 5FU in BC cell lines through decreasing the H-ras gene and protein expression, Rac-1 protein expression and Rho-A gene and protein expression which resulting in profound changes in cancerous cell phenotype as resistance to apoptosis and their adaptive ability to the surrounding environment.

Zhang et al. [39] have revealed that the treatment of gastric cancer cells with 5FU has markedly increased cellular apoptosis which enhanced by the knock down of PHGDH, down regulation of mRNA and protein levels of Bcl-2 and up-regulation of Bax and caspase3 levels.

Ki67 is a nuclear protein associated with cellular proliferation. It is expressed in S, G1, G2 and M phases of cell cycle but is non existing in G0. It shows low levels of expression (<3% of cells) in normal breast tissue and ER-negative cells *[40]*.

Ki67 provides predictive data regarding the response and prognosis of BC patients receiving neoadjuvant treatment. It could help in the selection of patients who are unable to be treated by chemotherapeutic agents as those with HER2-gene negative and hormone receptor negative with low proliferation index *[41]*.

Regarding proliferation, in the current study, treated SEC bearing mice with 5FU demonstrated notable decline in immunohistochemical ki67 expression as compared with untreated SEC bearing mice received vehicle.

In this context, the results of the present study are in harmony with Cancello et al.[42] who evaluated the ki67 expression with significant decrease post chemotherapeutics versus pre-chemotherapeutics and with Matsubara et al. [43] who defined the ki67 expression changes as a prognostic marker regardless of cancer subtype. Also, Sheri et al. [44] and Cabrera-Galeana et al. [45] who evidenced that patients without decrease in ki67 expression after chemotherapy had serious prognostic outcomes, more liable recurrence and mortality.

Angiogenesis is implicated in a wide range of healthy and diseased conditions. It is responsible for facilitating the outgrowth of endothelial cells, vasodilatation and increase vascular permeability *[46]*.

Mercurio et al. [47] has reported that VEGF roles in BC are not limited to angiogenesis only but also the VEGF signaling in cancer cells increase the cellular ability to evade apoptosis and increase tumor invasiveness and metastases.

Grimm et al. [48] and Madu et al. [49] have documented that the targeting of VEGF or hypoxia inducible factors (HIFs) have been considered an important treatment option for several malignancies including BC.

Regarding angiogenesis, the treated SEC bearing mice with 5 FU in the present study showed significant reduction in the immunohistochemical VEGF expression versus the untreated SEC bearing mice received vehicle. These results are in accordance with previous study of Jahani et al. [50] who revealed that 5FU mediated antiangiogenic effects on endothelial cells which were evidenced by the inhibition of NF-ƙβ a hyper activated pathway in most cancer cells with consequence down regulation of MMP-2,9 and VEGF expression.

Sitagliptin is a highly selective oral DPP-4 inhibitor that increases the bioavailability of GLP-1. It is also known with its anti-inflammatory and immunoregulatory properties *[51]*.

Several studies have revealed its cytoprotective properties through attenuating oxidative stress and improving mitochondrial dysfunction *[52]*. Based on all the afore mentioned premises, the inhibition of DPP-4 has been suggested to be of potential benefits for patients with breast cancer to modulate the chemotherapeutic anticancer activity and possess cytoprotective effects.

In the current study, the SEC bearing mice treated with free sitagliptin demonstrated notable decline in end tumor volume, non-significant changes in MDR-1 tissue levels, significant increase in caspase3 tissue levels, significant increase in GSH and significant decrease in MDA tissue levels, non-significant increase in tissue necrosis

percentage, significant decrease in ki67 tissue expression and significant decrease in VEGF tissue expression. These results substantiated that sitagliptin has anti-cancer properties.

In this context, the result of this study is in line with Hollande et al. [53] who observed the significant reduction of tumor growth and small tumor masses in mouse models of hepatocellular, breast and prostatic carcinomas when the intratumoral DPP-4 activity was inhibited with sitagliptin.

According to Chu et al. [54], sitagliptin is a substrate of hOAT-1, OATP4C1 and MDR1 transporter proteins at renal proximal tubules cells. They also indicate that sitagliptin is not a perpetrator of drug-drug interactions with P-gp, hOAT-1 or 3 substrates.

The obtained results are in agree with Kosowska et al. [55]who reported that sitagliptin modulated the production of apoptotic proteins and reduce the synthesis of proteins involved in metastatic process in ovarian cancer cell lines and with Sarkar et al. [56] who documented the apoptogenic behavior of sitagliptin in MCF7 breast cancer cell line and HepG2 liver cancer cell lines through the increased activity of caspase3 in both cell lines.

The results of the present study substantiated the idea that sitagliptin has antioxidant properties in BC tissue. these results are in accordance with Salah et al. [57] who revealed that sitagliptin demonstrated notable decline in MDA levels and significant increase in total antioxidant capacity (TAC) in SEC bearing mice.

Also, Khedr et al. [58] have proved the antioxidant effects of sitagliptin which were evidenced through the reduction of NOX-2 pro-oxidant enzyme levels, increased levels of SOD enzyme and declined levels of MDA the lipid peroxidation marker.

The present work substantiated the idea that sitagliptin has antiproliferative effects which was detected through the decreased expression of the nuclear protein ki67immune staining. These results are in line with Abd El-Fattah et al. [59] who documented the downregulation of ki67 mRNA expression in NDEA induced HCC treated with sitagliptin.

Zheng et al. [60] have proved the role of exosomal DPP4 in the angiogenesis induction by increasing the expression of periostin and activation of Smad signaling pathway indicating that DPP4 may be a promising anti-angiogenic targeted therapy and prognostic biomarker in cancer colon.

In the present study regarding the anticancer effects, the treated SEC bearing mice with either sitagliptin PLGA NPs or sitagliptin niosome NPs versus treated SEC bearing mice with free sitagliptin showed nonsignificant decrease in end tumor volume, nonsignificant decrease in MDR-1 tissue expression, significant increase in tissue caspase3, nonsignificant changes in GSH and MDA tissue levels, nonsignificant increase in tissue necrosis percentage and nonsignificant decrease in immune stained ki67 and VEGF tissue expression

To our knowledge, this is the first study to investigate the potential anti-cancerous effects of the combination therapy of 5FU and sitagliptin comparing with the effect of 5FU monotherapy.

Regarding their anticancer effects, the treated SEC bearing mice either with 5FU+ free sitagliptin, 5FU+ sitagliptin-PLGA NPs or 5FU+ sitagliptin-niosome NPs demonstrated notable decline in end tumor volume, significant increase in MDR-1levels, significant increase in caspase3 levels, significant increase in GSH and significant decrease in MDA levels, significant increase in the necrotic area percentage and significant decrease in the expression of immune stained ki67 and VEGF versus the SEC bearing mice treated with 5FU alone.

The significant increased levels of tumor tissue MDR1 and caspase3 were in accordance with Sakaeda et al.[61] and Buda et al. [62] who documented that the rapid upregulation of MDR1 mRNA was acellular protective mechanism against the increased apoptotic stimuli.

Nephrotoxicity is one of the most disrupting cytotoxic consequences of 5FU therapy. One of the aims of designing this study was to facilitate patients' adherence to 5FU in BC chemotherapy by preventing its nephrotoxic effects using sitagliptin.

In current study, it has been demonstrated that nephrotoxicity was indicated by elevated serum levels of BUN and creatinine in treated SEC bearing mice with 5FU as compared with untreated SEC bearing mice received vehicle

and these results were reflected to the histopathological examination of the kidney that showed renal tubular dilatation, tubular epithelial degeneration, chronic inflammatory cells infiltration and necrosis. This was in accordance with Famurewa et al. [63] who demonstrated the capability of 5FU to induce nephrotoxicity through the activation of oxidative stress, pro-inflammatory and caspase dependent apoptosis which was evident by elevated serum urea and creatinine levels.

Adikwu et al. [64] have reported that in addition to the alternation in serum renal function markers, the kidney redox state was also impaired which was evidenced by increase in MDA levels and decrease in CAT, SOD and GSH levels in renal tissue. These findings indicate the role of oxidative stress which affects the kidney ability to scavenge and neutralize free radicles predisposing it to various assaults.

In the current study, the treated SEC bearing mice with either sitagliptin free, sitagliptin PLGA NPs or sitagliptin niosome NPs showed non-significant changes in BUN and serum creatinine levels versus either normal control group or untreated SEC bearing mice received vehicle.

The treated SEC bearing mice with 5FU+free sitagliptin, 5FU+ sitagliptin-PLGA NPs or 5FU+ sitagliptin-niosome NPs demonstrated notable decline in serum BUN and creatinine levels versus treated SEC bearing mice with 5FU alone indicating the nephroprotective effects against 5FU-induced nephrotoxicity. These results were reflected to the histopathological findings that showed that sitagliptin ameliorated the glomerular and tubular damage induced by 5FU.

Loading sitagliptin either on PLGA or niosome NPS improved its nephroprotective properties which was evidenced by the significant decrease in serum BUN and the decrease in serum creatinine that was non-significant and histopathological findings versus free sitagliptin when combined with 5FU.

Sitagliptin niosome NPs showed better nephroprotective effects evidenced by significant decrease in serum BUN levels compared to sitagliptin PLGA NPs and improved the kidney histopathological findings as it showed normally shaped glomeruli and few atrophic glomeruli surrounded by normally shaped tubules focal hyalinization, no inflammation or necrosis.

The improvement of renal parameters by nano formulations may be due to improving the plasma level and stability of sitagliptin, thus need to be verified by further investigations.

Conclusions:

The addition of sitagliptin to 5FU in BC therapy showed encouraging results regarding magnitude its anticancer effects evidenced by decreased end tumor volume through augmenting its apoptotic, antioxidant, antiproliferative and antiangiogenic effects in SEC cells. Sitagliptin also possess nephroprotective effects evidenced by improving the renal parameters serum BUN and creatinine. The loading of sitagliptin on PLGA or niosome NPs improved its apoptotic properties in SEC cells and augment free sitagliptin nephroprotective effects.

Finally, the result of this study recommends the adjuvant use of sitagliptin with 5FU in BC therapy which could improve the anticancer effects and attenuates disrupting nephrotoxicity. However, these results have to be verified by further animal studies for longer duration and human clinical. Also, in-vitro investigations have to be conducted on sitagliptin nano formulations as a treatment modality.

Financial support and sponsorship:

Nil

Conflict of Interest:

Nil

References:

1. Badria F, Fathy H, Fatehe A, Elimam D, Ghazy M. Evaluate the cytotoxic activity of honey, propolis, and bee venom from different localities in Egypt against liver, breast, and colorectal cancer. J Apither. 2017;2:1-4.

2. Meral I, Pala M, Akbas F, Ustunova S, Yildiz C, Demirel MH. Effects of thymoquinone on liver miRNAs and oxidative stress in Ehrlich acid mouse solid tumor model. Biotech Histochem. 2018;93:301-8.

3. Amin AH, El-Missiry MA, Othman AI, Ali DA, Gouida MS, Ismail AH. Ameliorative effects of melatonin against solid Ehrlich carcinoma progression in female mice. J Pineal Res. 2019;67:e12585.

4. Liu XY, Zhang FR, Shang JY, Liu YY, Lv XF, Yuan JN, et al. Renal inhibition of miR-181a ameliorates 5-fluorouracil-induced mesangial cell apoptosis and nephrotoxicity. Cell Death Dis. 2018;9:610.

5. Akindele AJ, Oludadepo GO, Amagon KI, Singh D, Osiagwu DD. Protective effect of carvedilol alone and coadministered with diltiazem and prednisolone on doxorubicin and 5-fluorouracil-induced hepatotoxicity and nephrotoxicity in rats. Pharmacol Res Perspect. 2018;6.

6. Schetz M, Dasta J, Goldstein S, Golper T. Drug-induced acute kidney injury. Curr Opin Crit Care. 2005;11:555-65.

7. Almagthali AG, Alkhaldi EH, Alzahrani AS, Alghamdi AK, Alghamdi WY, Kabel AM. Dipeptidyl peptidase-4 inhibitors: Anti-diabetic drugs with potential effects on cancer. Diabetes Metab Syndr. 2019;13:36-9.

8. Tseng CH. Sitagliptin and pancreatic cancer risk in patients with type 2 diabetes. Eur J Clin Invest. 2016;46:70-9.

9. Rogalska A, Sliwinska A, Kasznicki J, Drzewoski J, Marczak A. Effects of epothilone A in combination with the antidiabetic drugs metformin and sitagliptin in HepG2 human hepatocellular cancer cells: role of transcriptional factors NF-κB and p53. Asian Pac J Cancer Prev. 2016;17:993-1001.

10. Haq Asif A, Harsha S, Hodalur Puttaswamy N, E. Al-Dhubiab B. An effective delivery system of sitagliptin using optimized mucoadhesive nanoparticles. Appl Sci. 2018;8:861.

11. Kabel AM, Atef A, Estfanous RS. Ameliorative potential of sitagliptin and/or resveratrol on experimentally-induced clear cell renal cell carcinoma. Biomed Pharmacother. 2018;97:667-74.

12. Jahangir MA, Khan R, Sarim Imam S. Formulation of sitagliptin-loaded oral polymeric nano scaffold: process parameters evaluation and enhanced anti-diabetic performance. Artif Cells Nanomed Biotechnol. 2018;46:66-78.

13. Choi YH, Han HK. Nanomedicines: current status and future perspectives in aspect of drug delivery and pharmacokinetics. J Pharm Investig. 2018;48:43-60.

14. Hegazi AG, Abdel-Rahman EH, Abd-Allah F, Abdou AM. Influence of honey on immune status in mice-bearing ehrlich carcinoma. J Clin Cell Immunol. 2015;6:1000295.

15. Gaballah HH, Gaber RA, Mohamed DA. Apigenin potentiates the antitumor activity of 5-FU on solid Ehrlich carcinoma: Crosstalk between apoptotic and JNK-mediated autophagic cell death platforms. Toxicol Appl Pharmacol. 2017;316:27-35.

16. Salah R, Salama MF, Mahgoub HA, El-Sherbini ES. Antitumor activity of sitagliptin and vitamin B12 on Ehrlich ascites carcinoma solid tumor in mice. J Biochem Mol Toxicol. 2021;35:e22645.

17. Essa D, Kondiah PP, Choonara YE, Pillay V. The design of poly (lactide-co-glycolide) nanocarriers for medical applications. Front Bioeng Biotechnol. 2020;8:48.

18. Sultan AA, El-Gizawy SA, Osman MA, El Maghraby GM. Peceosomes for oral delivery of glibenclamide: In vitro in situ correlation. J Drug Deliv Sci Technol. 2017;41:303-9.

19. Sultan AA, El-Gizawy SA, Osman MA, El Maghraby GM. Colloidal carriers for extended absorption window of furosemide. J Pharm Pharmacol. 2016;68:324-32.

20. El-Dayem SMA, Fouda FM, Ali EH, Motelp BAAE. The antitumor effects of tetrodotoxin and/or doxorubicin on Ehrlich ascites carcinoma-bearing female mice. Toxicol Ind Health. 2013;29:404-17.

21. Beutler E. Improved method for the determination of blood glutathione. J Lab Clin Med. 1963;61:882-8.

22. Ali DA, Badr El-Din NK, Abou-El-magd RF. Antioxidant and hepatoprotective activities of grape seeds and skin against Ehrlich solid tumor induced oxidative stress in mice. Egypt J Basic Appl Sci. 2015;2:98-109.

23. Othman AI, El-Sherbiny IM, ElMissiry MA, Ali DA, AbdElhakim E. Polyphenon-E encapsulated into chitosan nanoparticles inhibited proliferation and growth of Ehrlich solid tumor in mice. Egypt J Basic Appl Sci. 2018;5:110-20.

24. El-Sisi AE, Sokar SS, Ibrahim HA, Abu-Risha SE. Enhanced anticancer activity of combined treatment of imatinib and dipyridamole in solid Ehrlich carcinoma-bearing mice. Naunyn Schmiedebergs Arch Pharmacol. 2020:1-17.

25. Alessandra-Perini J, Perini JA, Rodrigues-Baptista KC, de Moura RS, Junior AP, Dos Santos TA, et al. Euterpe oleracea extract inhibits tumorigenesis effect of the chemical carcinogen DMBA in breast experimental cancer. BMC complementary and alternative medicine. 2018;18:1-11.

26. Maae E, Nielsen M, Steffensen KD, Jakobsen EH, Jakobsen A, Sørensen FB. Estimation of immunohistochemical expression of VEGF in ductal carcinomas of the breast. J Histochem Cytochem. 2011;59:750-60.

27. Tan P-H, Bay B-H, Yip G, Selvarajan S, Tan P, Wu J, et al. Immunohistochemical detection of Ki67 in breast cancer correlates with transcriptional regulation of genes related to apoptosis and cell death. Mod Pathol. 2005;18:374-81.

28. Schneider BP, Sledge GW, Jr. Drug insight: VEGF as a therapeutic target for breast cancer. Nat Clin Pract Oncol. 2007;4:181-9.

29. Ghiringhelli F, Apetoh L. Enhancing the anticancer effects of 5-fluorouracil: current challenges and future perspectives. Biomed J. 2015;38.

30. Arias JL. Novel strategies to improve the anticancer action of 5-fluorouracil by using drug delivery systems. Molecules. 2008;13:2340-69.

31. Soliman NA, Abd-Ellatif RN, AA EL, Shalaby SM, Bedeer AE. Luteolin and 5-flurouracil act synergistically to induce cellular weapons in experimentally induced Solid Ehrlich Carcinoma: Realistic role of P53; a guardian fights in a cellular battle. Chem Biol Interact. 2019;310:108740.

32. Jian-Hui Y, Cheng J-Q, Jiang L-Y, Wei-Dong J, Liang-Feng G, Jian-Jun L, et al. Breast cancer resistance protein expression and 5-fluorouracil resistance. Biomed Environ Sci. 2008;21:290-5.

33. Zhang F, Zhang H, Wang Z, Yu M, Tian R, Ji W, et al. P-glycoprotein associates with Anxa2 and promotes invasion in multidrug resistant breast cancer cells. Biochem Pharmacol. 2014;87:292-302.

34. Ma Y, Wang Y, Xu Z, Wang Y, Fallon JK, Liu F. Extreme low dose of 5-fluorouracil reverses MDR in cancer by sensitizing cancer associated fibroblasts and down-regulating P-gp. PLoS One. 2017;12:e0180023.

35. Inoue Y, Miki C, Watanabe H, Hiro J, Toiyama Y, Ojima E, et al. Schedule-dependent cytotoxicity of 5-fluorouracil and irinotecan in a colon cancer cell line. J Gastroenterol. 2006;41:1149-57.

36. Ke H, Wang X, Zhou Z, Ai W, Wu Z, Zhang Y. Effect of weimaining on apoptosis and Caspase-3 expression in a breast cancer mouse model. J Ethnopharmacol. 2021;264:113363.

37. Yang X, Zhong D-N, Qin H, Wu P-R, Wei K-L, Chen G, et al. Caspase-3 over-expression is associated with poor overall survival and clinicopathological parameters in breast cancer: a meta-analysis of 3091 cases. Oncotarget. 2018;9:8629.

38. Ponce-Cusi R, Calaf GM. Apoptotic activity of 5-fluorouracil in breast cancer cells transformed by low doses of ionizing α-particle radiation. Int J Oncol. 2016;48:774-82.

39. Zhang Y, Yang L, Dai G, Cao H. Knockdown of PHGDH potentiates 5-FU cytotoxicity in gastric cancer cells via the Bcl-2/Bax/caspase-3 signaling pathway. Int J Clin Exp Pathol. 2018;11:5869-76.

40. Inwald E, Klinkhammer-Schalke M, Hofstädter F, Zeman F, Koller M, Gerstenhauer M, et al. Ki-67 is a prognostic parameter in breast cancer patients: results of a large population-based cohort of a cancer registry. Breast Cancer Res Treat. 2013;139:539-52.

41. Fasching PA, Heusinger K, Haeberle L, Niklos M, Hein A, Bayer CM, et al. Ki67, chemotherapy response, and prognosis in breast cancer patients receiving neoadjuvant treatment. BMC cancer. 2011;11:1-13.

42. Cancello G, Bagnardi V, Sangalli C, Montagna E, Dellapasqua S, Sporchia A, et al. Phase II Study With Epirubicin, Cisplatin, and Infusional Fluorouracil Followed by Weekly Paclitaxel With Metronomic Cyclophosphamide as a Preoperative Treatment of Triple-Negative Breast Cancer. Clin Breast Cancer. 2015;15:259-65.

43. Matsubara N, Mukai H, Masumoto M, Sasaki M, Naito Y, Fujii S, et al. Survival outcome and reduction rate of Ki-67 between pre- and post-neoadjuvant chemotherapy in breast cancer patients with non-pCR. Breast Cancer Res Treat. 2014;147:95-102.

44. Sheri A, Smith IE, Johnston SR, A'Hern R, Nerurkar A, Jones RL, et al. Residual proliferative cancer burden to predict long-term outcome following neoadjuvant chemotherapy. Ann Oncol. 2015;26:75-80.

45. Cabrera-Galeana P, Muñoz-Montaño W, Lara-Medina F, Alvarado-Miranda A, Pérez-Sánchez V, Villarreal-Garza C, et al. Ki67 Changes Identify Worse Outcomes in Residual Breast Cancer Tumors After Neoadjuvant Chemotherapy. Oncologist. 2018;23:670-8.

46. Schneider BP, Sledge GW. Drug insight: VEGF as a therapeutic target for breast cancer. Nat Clin Pract Oncol. 2007;4:181-9.

47. Mercurio AM, Lipscomb EA, Bachelder RE. Non-angiogenic functions of VEGF in breast cancer. J Mammary Gland Biol Neoplasia. 2005;10:283-90.

48. Grimm D, Wehland M, Pietsch J, Infanger M, Bauer J. Drugs interfering with apoptosis in breast cancer. Curr Pharm Des. 2011;17:272-83.

49. Madu CO, Wang S, Madu CO, Lu Y. Angiogenesis in Breast Cancer Progression, Diagnosis, and Treatment. J Cancer. 2020;11:4474-94.

50. Jahani M, Azadbakht M, Rasouli H, Yarani R, Rezazadeh D, Salari N, et al. L-arginine/5-fluorouracil combination treatment approaches cells selectively: Rescuing endothelial cells while killing MDA-MB-468 breast cancer cells. Food Chem Toxicol. 2019;123:399-411.

51. Solerte SB, D'Addio F, Trevisan R, Lovati E, Rossi A, Pastore I, et al. Sitagliptin treatment at the time of hospitalization was associated with reduced mortality in patients with type 2 diabetes and COVID-19: a multicenter, case-control, retrospective, observational study. Diabetes care. 2020;43:2999-3006.

52. Abuelezz SA, Hendawy N, Abdel Gawad S. Alleviation of renal mitochondrial dysfunction and apoptosis underlies the protective effect of sitagliptin in gentamicin-induced nephrotoxicity. J Pharm Pharmacol. 2016;68:523-32.

53. Hollande C, Boussier J, Ziai J, Nozawa T, Bondet V, Phung W, et al. Inhibition of the dipeptidyl peptidase DPP4 (CD26) reveals IL-33-dependent eosinophil-mediated control of tumor growth. Nat Immunol. 2019;20:257-64.

54. Chu XY, Bleasby K, Yabut J, Cai X, Chan GH, Hafey MJ, et al. Transport of the dipeptidyl peptidase-4 inhibitor sitagliptin by human organic anion transporter 3, organic anion transporting polypeptide 4C1, and multidrug resistance P-glycoprotein. J Pharmacol Exp Ther. 2007;321:673-83.

55. Kosowska A, Garczorz W, Kłych-Ratuszny A, Aghdam MRF, Kimsa-Furdzik M, Simka-Lampa K, et al. Sitagliptin Modulates the Response of Ovarian Cancer Cells to Chemotherapeutic Agents. Int J Mol Sci. 2020;21.

56. Sarkar M, Dey S, Giri B. Antiproliferative and apoptogenic efficacy of antidiabetic drugs metformin and sitagliptin against MCF7 and HEPG2 cancer cells: a comparative molecular study. J Drug Deliv Ther. 2017;7:11-21.

57. Salah R, Salama MF, Mahgoub HA, El-Sherbini ES. Antitumor activity of sitagliptin and vitamin B12 on Ehrlich ascites carcinoma solid tumor in mice. J Biochem Mol Toxicol. 2021;35:e22645.

58. Khedr R, Ahmed A, Kamel R, Rafaat E. Antioxidant effects of sitagliptin in a rat model of intestinal ischemia/reperfusion injury. J Adv Pharm Res. 2021;5:234-40.

59. Abd El-Fattah EE, Saber S, Youssef ME, Eissa H, El-Ahwany E, Amin NA, et al. AKT-AMPKα-mTOR-dependent HIF-1α Activation is a New Therapeutic Target for Cancer Treatment: A Novel Approach to Repositioning the Antidiabetic Drug Sitagliptin for the Management of Hepatocellular Carcinoma. Front Pharmacol. 2021;12:720173.

60. Zheng X, Liu J, Li X, Tian R, Shang K, Dong X, et al. Angiogenesis is promoted by exosomal DPP4 derived from 5-fluorouracil-resistant colon cancer cells. Cancer Lett. 2021;497:190-201.

61. Sakaeda T, Nakamura T, Hirai M, Kimura T, Wada A, Yagami T, et al. MDR1 Up-Regulated by Apoptotic Stimuli Suppresses Apoptotic Signaling. Pharm Res. 2002;19:1323-9.

62. Buda G, Orciuolo E, Maggini V, Galimberti S, Barale R, Rossi AM, et al. MDR1 modulates apoptosis in CD34+ leukemic cells. Ann Hematol. 2008;87:1017-8.

63. Famurewa AC, Asogwa NT, Aja PM, Akunna GG, Awoke JN, Ekeleme-Egedigwe CA, et al. Moringa oleifera seed oil modulates redox imbalance and iNOS/NF-κB/caspase-3 signaling pathway to exert antioxidant, anti-inflammatory and antiapoptotic mechanisms against anticancer drug 5-fluorouracil-induced nephrotoxicity in rats. S Afr J Bot. 2019;127:96-103.

64. Adikwu E, Ebinyo N, Amgbare B. Protective activity of selenium against 5-fluorouracil-induced nephrotoxicity in ratsprotective activity of selenium against 5-fluorouracil-induced hepatotoxicity in rats. Cancer Transl Med. 2019;5:50.